INTERNATIONAL JOURNAL OF ENERGY STUDIES

e-ISSN: 2717-7513 (ONLINE); homepage: https://dergipark.org.tr/en/pub/ijes

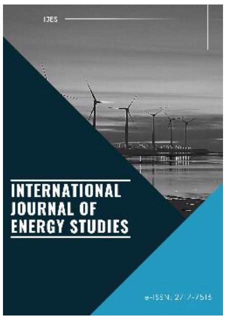

Research Article

Int J Energy Studies 2023; 8(3): 491-512

DOI: 10.58559/ijes.1264797

Received	:	14 Mar 2023
Revised	:	12 June 2023
Accepted	:	14 June 2023

Numerical investigation of the effect of operating conditions on the performance parameters of PEM fuel cells

Kemal Bilen[a*], **Batukan Cem Tarhan**[b], **Selahattin Çelik**[c]

[a] *Ankara Yıldırım Beyazıt University, Faculty of Engineering and Natural Sciences, ORCID: 0000-0003-1775-7977*
[b] *Ankara Yıldırım Beyazıt University, Graduate School of Natural and Applied Sciences, ORCID: 0000-0002-3800-503X*
[c] *Ankara Yıldırım Beyazıt University, Faculty of Engineering and Natural Sciences, ORCID: 0000-0002-7306-9784*
*(*Corresponding Author: kemal.bilen@aybu.edu.tr)*

Highlights

- The operating conditions of the PEM fuel cell, which is one of the fuel cells, were evaluated.
- The temperature value in the PEM fuel cell is discussed.
- The pressure value in the PEM fuel cell is discussed.
- While the performance of a PEM fuel cell increases with the operating temperature, it starts to decrease after 90 °C.

You can cite this article as: Bilen K, Tarhan BC, Çelik S. Numerical investigation of the effect of operating conditions on the performance parameters of PEM fuel cells. Int J Energy Studies 2023; 8(3): 491-512.

ABSTRACT

The operating parameters of proton exchange membrane fuel cells (PEMFCs) are very effective at generating heat. The study examined and evaluated parameters that can help determine fuel cell (FC) performance. The parameters and structures used in systems have been examined. In this context, performance evaluations have been made by performing electrochemical analyses of PEMFCs. Evaluations about how the study parameters affect the performance was made on MATLAB® and the results were presented. As a result of the study, it was seen that the operating temperature increased the efficiency until it reached certain limits. On the other hand, although the performance-enhancing effects of the working pressure are observed, high pressure appears as an obstacle. Air stoichiometric rate is another variable that affects FC performance. While high stoichiometric rates improve performance, they can adversely affect the membrane. According to the simulation result, it was found that the working temperature, working pressure and air stoichiometry should be optimized together.

Keywords: Fuel cell, FC, Electrochemical analysis, Polymer electrolyte membrane, PEMFC, Fuel cell modeling, Polarization curves

1. INTRODUCTION

Fuel cells convert chemical energy into electrical energy and do this with high efficiency and zero emission and they have attracted the world’s attention with these features in recent years. The energy need of the world increases by approximately 1.8% every year [1]. Also, alternative energy producers such as FCs have gained importance due to the rapid increase in pollution and a decrease in fossil fuel reserves globally in the last 40-50 years [2].

Fuel cells appear as one of the best solutions for this because of their properties. Fuel cells attract attention because they have a high-power density of up to three times compared to batteries and are longer lasting. In addition, in the last five years, hydrogen FC electric cars have emerged in the previous five years. Fuel cells have passed more than a century since their first discovery. Srinivasan [3] and Thomas et al. [4] referred to the history of FCs. The basis of FCs was first described by Christian Schoenbein in 1838. In 1842, Sir William Grove discovered the first FC prototype, which operates according to the opposite principle of water electrolysis. The first 5 kW alkaline FC was introduced to the world by Francis Bacon in 1950. Sunden [5] mentioned the practical application of FCs. It was first used in space exploration in the Gemini project in the 1960s. The use of Proton Exchange Membrane Fuel Cells (PEMFCs) in NASA’s space projects started around this time.

Today, a large portion of energy consumption is in the field of transportation. Fuel cells have the potential to subsidize a large portion of this energy need. For this reason, research on FCs that can be used in portable vehicles is increasing.

A fuel cell generates electricity from the chemical energy of the fuel electrochemically and directly. Electrochemical reactions are used in conventional batteries as well as FCs. However, FCs do not need to be recharged like a battery, as long as fuel and oxidant continue to supply. PEMFCs are low-temperature FCs that use a solid polymer in the form of a solid phase proton conducting membrane as an electrolyte which eliminates the need to contain corrosive liquids. PEMFCs have many advantages over the other FC types, including low-temperature operation, high power density, fast start-up, system robustness, flexibility of fuel type (with reformer), and reduced sealing, corrosion, shielding, or leaking concerns [6]. In this case, the most advantageous fuel cell type is PEMFC, thanks to its portability and low-temperature operation [7, 8].

A schematic diagram of the operating principle and chemical reactions of a PEM fuel cell is shown in Fig. 1.

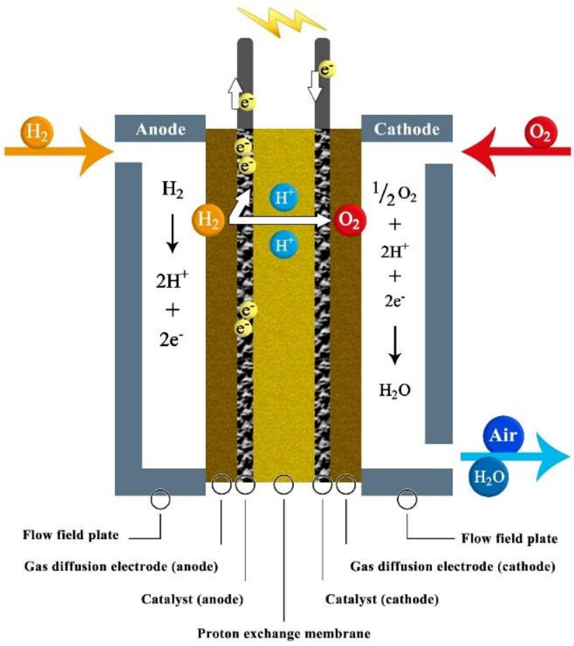

Figure 1. Schematic diagram of operating principle and chemical reactions of PEMFC (adapted from reference 9).

The performance parameters of PEMFCs can be improved using cooling of the cells. Therefore, many researchers have focused on the cooling of the PEMFCs and several studies can be found about the cooling of the FCs in the literature. Many studies have shown that the increase in the system costs is due to the lack of analysis of the operating parameters of the FCs. Correct selection of the parameters provides technical and economic benefits. In a theoretical study, Sankar et al. [10] used cooling fans to keep the operating temperature of the FC constant. In the study, it is shown that fans controlled by a nonlinear sliding mode supplied better results than fans moving at a specific rate. Also, the constant temperature had a positive effect on the system.

Heat spreaders execute passive cooling of the FCs. In order to achieve a high heat transfer rate, it is crucial to choose materials with high thermal properties. In addition to being with good thermal properties, it makes the FC more stable. In another experimental study performed by Faghri and Guo [11], passive cooling was obtained with heat pipes as heat spreaders. In the study, the high thermal conductivity of the heat pipes has been compared with other materials and satisfying results have been achieved by using heat pipes. In addition, the operating temperature was stabilized.

Two-phase heat transfer has the highest heat removal capacity. In this cooling method, a large amount of heat exchange is essential. Since the operating temperature of PEMFCs is between 60 and 80 degrees, the working fluid must undergo phase change in this temperature range. In an experimental study, Choi et al. [12] used HFE 7100 for cooling of PEMFCs. According to experimental data, two-phase cooling was functional and kept the temperature below 63 °C. Afshari et al. [13] examined the performance difference between two different types of geometry (straight and zigzag) in a numerical study. Zigzag ducts reduce heat dissipation by 8% while reducing temperature difference by 23% and the maximum temperature by 5%. Thus, the decreasing temperature rose the FC performance and life.

Han et al. [14] theoretically showed thermal management is a vital factor for better FC performance. In the modelled system, the heat generation and cooling module analysed on the MATLAB® platform are essential for performance analysis. Hajmohammedi and Toghraei [15] showed in their numerical study that aluminium-containing water significantly increases its thermal conductivity. In addition, the use of nanofluids significantly reduces the size of the cooling systems. Amount of nanoparticles added to the coolant affects the cooling capacity.

Yu and Jung [16] investigated the control of heat management in the system with different algorithms in their theoretical study. As a result of the research, it was observed that the coolant temperature and FC temperature are the main factors of the performance. The return control algorithm has been determined as the most useful algorithm.

Saygili et al. [17] numerically examined different liquid cooling mechanisms in their tests using a 3 kW PEMFC, three various mechanisms were analyzed, and their performances were tried to be increased with different control mechanisms. As a result of the modelling and analysis on MATLAB®, it is understood that the mechanism and algorithm used have an essential place in the performance of FCs.

In PEMFCs, the optimum operating temperature and regular heat distribution protect the FCs and the system for a longer operating time. Besides, it directly affects FC performance. Various factors affect efficiency. Among these factors, FC size, system complexity, the amount of heat removed from the system, and operating parameters are essential. Theoretical research by Fronk et al. [18] has shown that in a FC where the operating temperature is between 80 °C and 90 °C, the working pressure reaches 3 atm, and the radiator size should be 1.5 times larger than the internal combustion engine producing the same power.

The efficiency of FCs is highly dependent on operating temperature. High temperature causes membrane dehydration and stack degradation. The stability of a certain temperature is crucial in terms of providing maximum efficiency. The distribution of the temperature in a regular profile is vital in terms of both performance and durability as well as being stable. Therefore, heat generated by the losses must be adequately removed from the system. The removal of heat from the system can be achieved by conduction, natural convection, forced convection, and radiation. Heat transfer mechanisms are required to transfer the heat generated in the FC system to the external environment. In addition, the gases and water formed in the system provide to remove some of the heat.

Recent studies have shown that PEMFC's energy and exergy analysis are essential for the decision of FCs' performance. Nyugen et al. [19] made the exergy analysis of a PEMFC system with a heat recovery system with PEMFC. They created a computer model to increase the performance of the system. In a theoretical study carried out by Rahimi et al. [20], the wind turbine combined the FC system and obtained the hydrogen required for the FC from wind energy. Mert et al. [21] performed parametric research and made energy and exergy analyses of PEMFC used in vehicles. The thermodynamic analysis was applied to the compressor humidifier pressure controller, cooling system, and FC cells. As a result, an exergy efficiency of 8% was obtained. Zafar and Dinçer [22] theoretically analyzed the wind turbine, PV, and FC system and they found their energy and exergy efficiencies.

As can be seen from the studies in the literature, numerical studies in fuel cells are carried out on the change on a limited parameter. Therefore, the aim of the present study is to numerically investigate the effect of operating conditions on the performance parameters of PEM fuel cells in a wide range of parameters. In the study, the effect of operating temperature, operating pressure, and stoichiometric rate on the voltage, current density, heat generation, and electrical efficiency of the PEM fuel cell was determined. In the study also, polarization curves at different operating temperatures, operating pressure, and stoichiometric rate were obtained.

2. ELECTROCHEMICAL ANALYSIS

Total cell voltage is calculated as the difference between the reversible and irreversible cell voltage. Reversible, that is, the maximum voltage is obtained using the Nernst equation from Mann et al. [23].

$$V_{\mathrm{rev}} = \frac{-\Delta G^{\circ}}{n_{\mathrm{e}}F} + \frac{RT_{\mathrm{FC}}}{n_{\mathrm{e}}F}\ln\left(\frac{p_{\mathrm{H_2}}\sqrt{p_{\mathrm{O_2}}}}{p_{\mathrm{H_2O}}^{\mathrm{sat}}}\right) \tag{1}$$

Where, $p_{\mathrm{H_2O}}^{\mathrm{sat}}$ is water vapor saturation pressure. $p_{\mathrm{H_2O}}^{\mathrm{sat}}$ can be approximated by the equation given by Musio et al. [24] and Miansari et al. [25]:

$$\log_{10} p_{\mathrm{H_2O}}^{\mathrm{sat}}(T_{\mathrm{FC}}) = -2.1794 + 0.02953T_{\mathrm{FC}} - 9.1837{T_{\mathrm{FC}}}^2 + 1.4454{T_{\mathrm{FC}}}^3 \tag{2}$$

T_{FC} is in Kelvin's unit. $p_{\mathrm{H_2}}$ and $p_{\mathrm{O_2}}$ are the partial pressure of H_2 and O_2. Rowe and Li [26] used the equations for the calculation of partial pressures H_2 and O_2 as follows:

$$p_{\mathrm{H_2}} = \frac{1 - X_{\mathrm{H_2O,A}}}{1 + (\frac{X_{\mathrm{A}}}{2})(\frac{1+\xi_{\mathrm{A}}}{\xi_{\mathrm{A}} - 1})} p_{\mathrm{A}} \tag{3}$$

$$p_{\mathrm{O_2}} = \frac{1 - X_{\mathrm{H_2O,C}}}{1 + (\frac{X_{\mathrm{C}}}{2})(\frac{1+\xi_{\mathrm{C}}}{\xi_{\mathrm{C}} - 1})} \tag{4}$$

Here, $X_{\mathrm{H_2O}}$ is the molar ratio of water and it is calculated as follows:

$$X_{\mathrm{H_2O}} = \frac{p_{\mathrm{H_2O}}^{\mathrm{sat}}}{p_{\mathrm{operating}}} \tag{5}$$

Using the Nernst equation developed by Amphlett et al. [27], the reversible voltage is calculated.

$$V_{\mathrm{rev}} = 1.229 - 8.5\cdot 10^{-4}(T_{\mathrm{FC}} - 298.25) + 4.3085\cdot 10^{-5} T_{\mathrm{FC}}\left[\ln\left(p_{\mathrm{H_2}}\right) + \frac{1}{2}\ln\left(p_{\mathrm{O_2}}\right)\right] \tag{6}$$

2.1. Voltage Losses

The operating voltage is obtained when the voltage losses, i.e., the sum of the irreversible voltage, are subtracted from the reversible voltage. The operating voltage is never constant because it is calculated due to the losses that change with the change of parameters such as operating temperature and current density. It consists of irreversible voltage, activation energy, ohmic losses, and concentration losses.

$$V_{\mathrm{operating}} = V_{\mathrm{rev}} - V_{\mathrm{irrev}} \tag{7}$$

$$V_{\mathrm{operating}} = V_{\mathrm{rev}} - (V_{\mathrm{act}} + V_{\mathrm{ohmic}} + V_{\mathrm{conc}}) \tag{8}$$

2.2. Activation Losses

Losses caused by low reaction rates at the anode and cathode are called activation losses. Activation losses can be calculated using empirical models developed by Amphlett et al. [27].

$$V_{\mathrm{act}} = -\left[\xi_1 + \xi_2 T_{\mathrm{FC}} + \xi_3 T_{\mathrm{FC}}\left[\ln\left(c'_{\mathrm{O}_2}\right)\right] + \xi_4 T_{\mathrm{FC}}[\ln(i)]\right] \tag{9}$$

In Eq. 9, ξ_x is the parametric coefficients, and it is taken as follows:

$$\xi_1 = -0.948$$
$$\xi_2 = 0.00286 + 0.0002\ln(A) + 4.3\cdot10^{-5}\ln\left(c'_{\mathrm{H}_2}\right)$$
$$\xi_3 = 7.6\cdot10^{-5}$$
$$\xi_4 = -1.93\cdot10^{-4}$$

where A is the fuel cell area in cm^2. Oxygen and hydrogen concentration at the cathode and anode could be calculated by Henry's law given by Amphlett et al. [27].

$$c'_{\mathrm{O}_2} = p_{\mathrm{O}_2} 1.97\cdot10^{-7}\exp\left(\frac{498}{T_{\mathrm{FC}}}\right) \tag{10}$$

$$c'_{\mathrm{H}_2} = p_{\mathrm{H}_2} 9.174\cdot10^{-7}\exp\left(\frac{-77}{T_{\mathrm{FC}}}\right) \tag{11}$$

2.3. Ohmic Losses

The losses in the fuel cell are generally caused by electrical resistance. Ohmic losses may have many reasons such as contact potential, electrode resistance, or membrane resistance. Since these values are difficult to pinpoint precisely, their value is found using empirical expressions.

There is a direct relationship between current and ohmic losses. The ohmic effect that occurs on fuel cell membranes is calculated:

$$V_{\text{ohmic}} = iR_{\text{int}} \tag{12}$$

Here, R_{int} given by Mann et al. [23] is the resistivity of the membrane and described as

$$R_{int} = \frac{\gamma_{\text{M}} l_{\text{mem}}}{A_{int}} \tag{13}$$

γ_{M} is calculated via the equation developed by Mann et al. [23].

$$\gamma_{\text{M}} = \frac{181.6\left[1 + 0.03\left(\frac{i}{A}\right) + 0.062\left(\frac{T_{\text{FC}}}{303}\right)^{2}\left(\frac{i}{A}\right)^{2.5}\right]}{\left[\lambda - 0.634 - 3\left(\frac{i}{A}\right)\right]\exp\left[4.18\left(\frac{T_{\text{FC}} - 303}{T_{\text{TF}}}\right)\right]} \tag{14}$$

In the equation, λ is a function of membrane moisture and depends on factors such as anode inlet gas rate. Its value is often set as the ideal value of 14 and can range from 14 to 22.

2.4. Concentration Losses

Concentration losses are losses caused by mass transfer limitations. These are formed between substances and products that react at high current densities. It affects the anode and cathode surfaces. Concentration losses are calculated by the following equation given by Spiegel [28].

$$V_{\text{conc}} = \frac{RT}{nF}\ln\left(\frac{J_{\text{L}}}{J_{\text{L}} - J}\right) \tag{15}$$

J_L takes a value between 1.6 and 2. However, the equation is valid only when the $J < J_L$ statement is implemented.

2.5. Fuel Cell Voltage Efficiency

The ideal fuel cell voltage corresponds to 1.481 V when the high-heating enthalpy is converted. When the output voltage of the fuel cell is divided by this value, the electrical efficiency of the fuel cell is calculated using Eq. 16 mentioned by Barbir [29].

$$\eta_{\mathrm{FC}} = \frac{V_{\mathrm{operating}}}{V_{\mathrm{HHV}}} = \frac{V_{\mathrm{operating}}}{1.481} \tag{16}$$

2.6. PEMFC Heat Generation

Heat generation due to losses can be found using Eq. 17. Here, $\dot{W}_{\mathrm{FC}}$ is the power generation of the fuel cell.

$$\dot{Q}_{\mathrm{gen}} = \dot{W}_{\mathrm{FC}} \left(\frac{V_{\mathrm{rev}}}{V_{\mathrm{operating}}} - 1 \right) \tag{17}$$

3. RESULTS AND DISCUSSION

In this study, performance changes of the PEM fuel cell were analyzed numerically using the MATLAB® program. Analyses were made based on theoretical equations, empirical equations, and various physical facts and concluded that the parametric model is an excellent way to predict fuel cells’ performance. A flowchart about numerical analysis for MATLAB® is shown in Fig. 2.

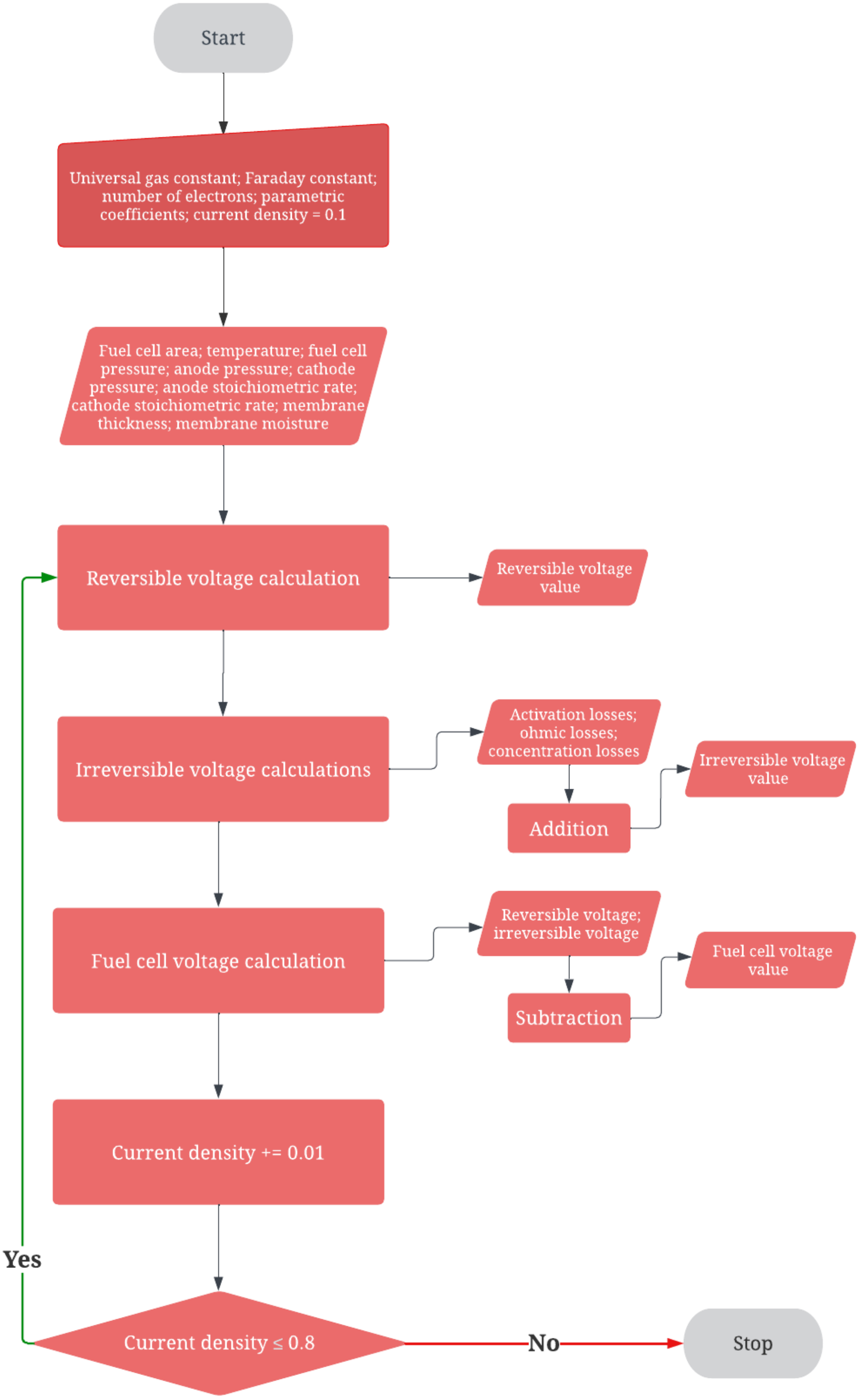

Figure 2. Flowchart for MATLAB®.

The analysis has been made by integrating some articles and applied based on the operating temperature, the operating pressure, and stoichiometric rates of the fuel cell. The conditions used are given in Table 1.

Table 1. The values range of the PEMFC.

Parameter	Value
Universal gas constant	8.3145 J/(mol·K)
Faraday's constant	96485 C/mol
Operating temperature	50 °C to 100 °C
Current density	0.1 A/cm^2 to 0.8 A/cm^2
Operating pressure	1 bar to 5 bar
Anode pressure	3 bar
Cathode pressure	3 bar
Anode stoichiometric rate	1 to 5
Cathode stoichiometric rate	1 to 5
Membrane thickness	0.005 cm
Fuel cell area	50 cm^2

Some polarization curves were compared with the results of some experimental and theoretical studies placed in the literature for the same temperature, pressure, and stoichiometric rate to verify the results of this study in Fig. 3. Firstly, results of this study were compared with Laurencelle et al.'s [30] study. Difference between the results was due to variations in factors such as the working area and gas pressure in the channel. Despite this difference, both studies have a similar rate of change in the fuel cell voltage with an increasing current density. Results of this study were also compared with Tohidi et al.'s [31] research and similar voltage values were observed with a corresponding rate of change in the polarization curves. Compared with Yan et al.'s [32] similar search, the results were found to be parallel. Within this study, the influence of stoichiometry was also examined, and the numerical outcomes were compared to those of Cellek and Bilgili's [33] work.

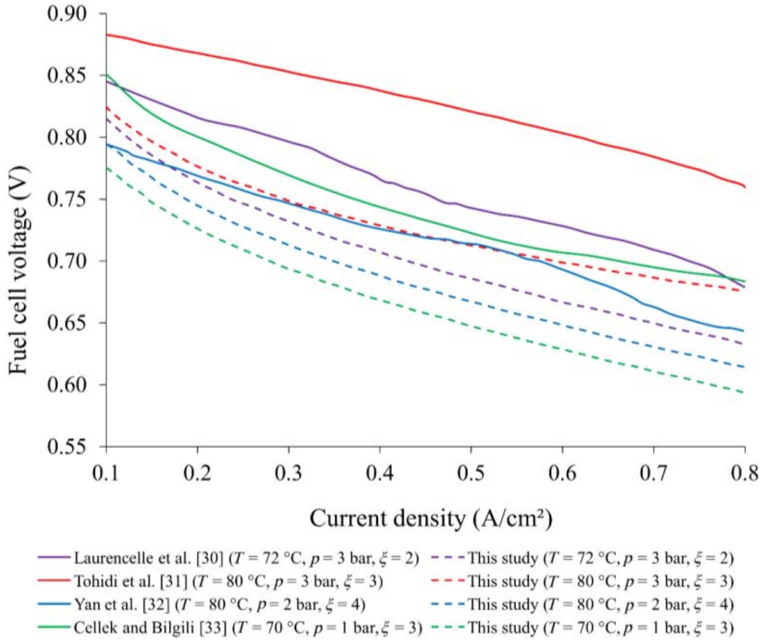

Figure 3. Comparison of the polarization curves with some previous experimental and theoretical studies [30-33].

Upon comparison, it was discerned that the studies exhibited a marked similarity. These comparisons between this study and previous studies placed in the literature indicate that the numerical approach of this study is consistent with the previous experimental and numerical research.

Electrochemical analysis has been done in fuel cells, and losses have been investigated. It has been observed that the losses in these cells are generally examined under three headings. Calculations of major losses are shown. The amount of heat generated due to losses was also calculated. The polarization curves of the fuel cell are shown in Fig. 4a depending on the operating temperature. The polarization curves of the fuel cell are also shown with bars in Fig. 4b for a clear representation. In this study, performance and efficiency of the cells in a certain temperature range were analyzed parametrically. Temperature range has been chosen between 50 °C and 100 °C because the operating temperature mentioned by Sunden of the low-temperature proton exchange membrane fuel cell remains between these values. The polarization curves of the fuel cell are shown as bars in Fig. 4b depending on the operating temperature for a clear representation.

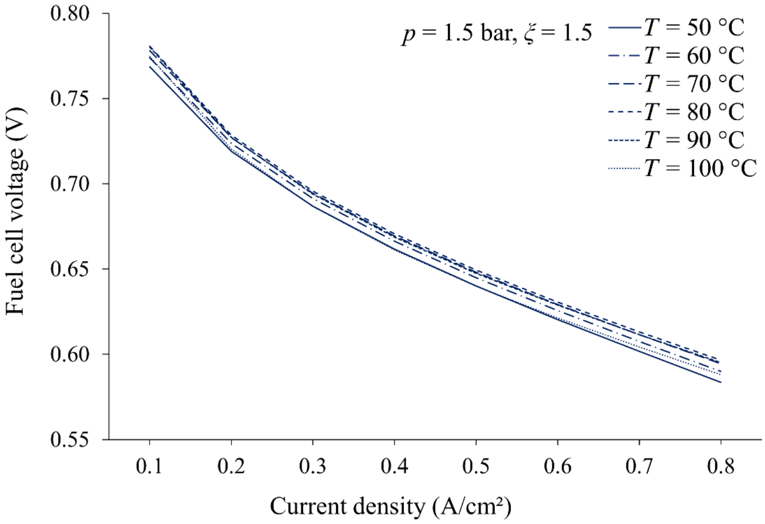

Figure 4a. Polarization curves at different operating temperatures.

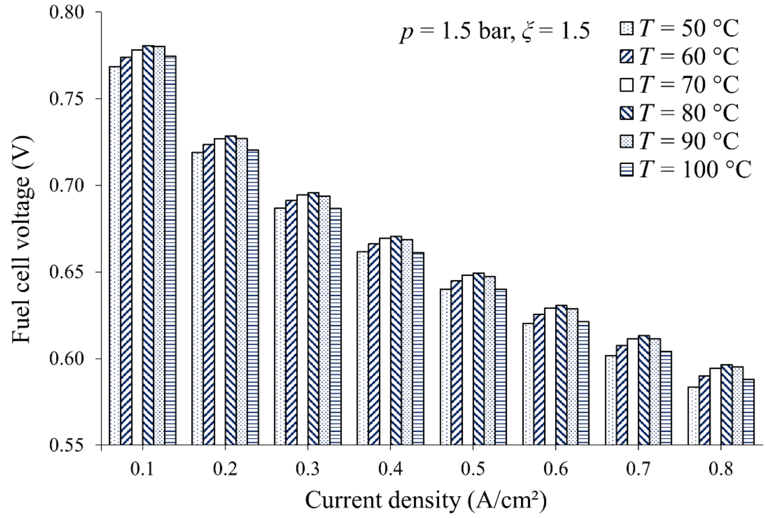

Figure 4b. Variation of fuel cell voltage with current density at different operating temperatures.

As a result of the analysis, the optimum operating temperature has been reached, and the system shown in Fig. 4a and Fig 4b has shown the optimum performance at 80 °C. The temperature must be kept at a specific value for the system to operate at high efficiency and durability. When sufficient humidity is provided in the PEMFC, the best performance is obtained at 80 °C. According to the Nernst equation (Eq. 1), voltage (V_{rev}) decreases as the temperature increases. Normally it can be thought that the performance should decrease with increasing temperature. However, with increasing temperature, the ion transfer rate also increases and the performance increase is more than the loss with temperature, and as a result, the performance of the fuel cell increases. Since the upper limit of the working strength of the polymer electrolyte membrane is 90 °C, the temperature was not increased further for this fuel cell type.

Operating pressure is another factor affecting efficiency in fuel cells. The increase in operating pressure positively affects the fuel cell voltage as shown in Fig. 5a, 5b, and 5c. Also, several negative effects referred to Tohidi et al. [31], such as high crossover, sealing problems, parasitic power loss, and higher cost for compression could be a challenge to increase operating pressure. The fuel cell efficiency must be increased by determining the optimum value of the pressure.

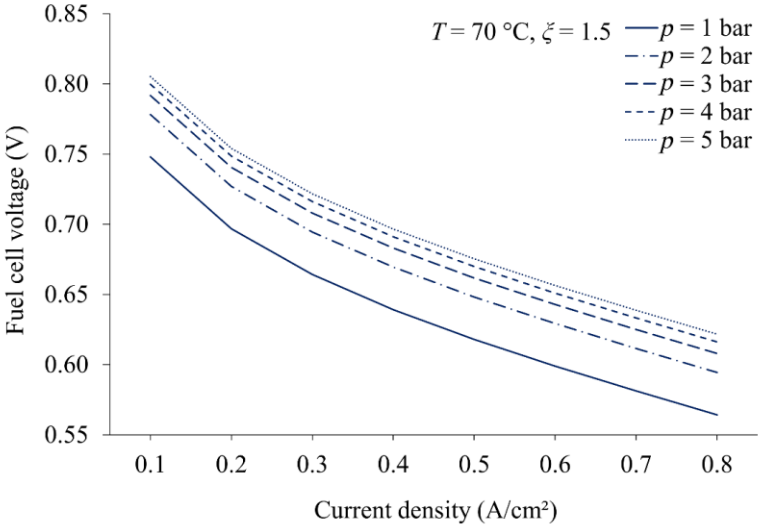

(a)

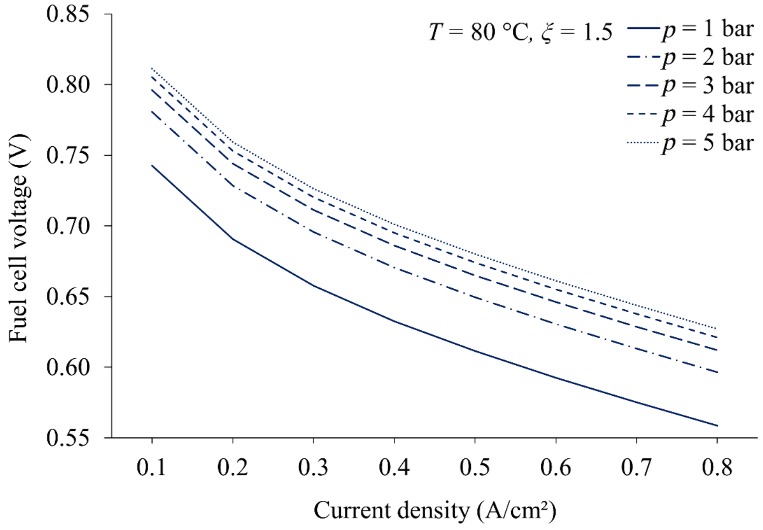

(b)

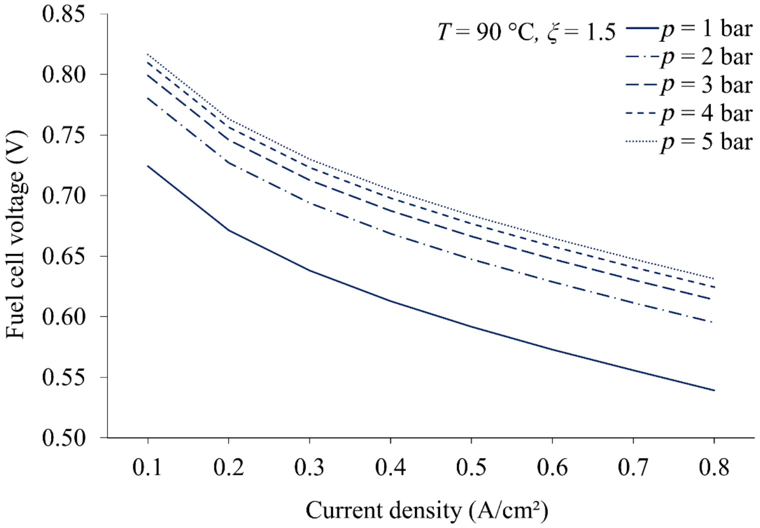

(c)

Figure 5. Variation of fuel cell voltage with current density at different pressure and temperatures: **a)** 70˚C **b)** 80˚C **c)** 90˚C.

It is seen that the fuel cell performance changes significantly with the change in pressure. As seen in Fig. 5, while performance increases rapidly up to 3 bar pressure, its effect on performance decreases at subsequent pressures. With increasing pressure, voltage (V_{rev}) increases according to the Nernst equation (Eq. 1). Thus, fuel cell performance increases with increasing pressure. However, in practice, ambient air is sent to the cathode side and additional power loss is required for additional pressurization. Therefore, operating the fuel cell at ambient pressure may be more effective in systems using hydrogen/air. In fuel cell systems using hydrogen/oxygen (such as submarine systems), the pressure value is used as 3 bar. Further pressurization may cause rupture of the membrane used in the fuel cell and mixing of fuel and oxidant, gas leaks and dangerous explosions. Cathode pressure is one of the factors affecting fuel cell performance and it was taken as a 3 bar in the study.

Another parameter affecting the fuel cell voltage is the feed gas stoichiometric rate. Changing of polarization curves with gas stoichiometric rate at specified temperature and pressure are presented in Fig. 6. Figures 6a, 6b, 6c, and 6d show in which direction the values affect the fuel cell voltage.

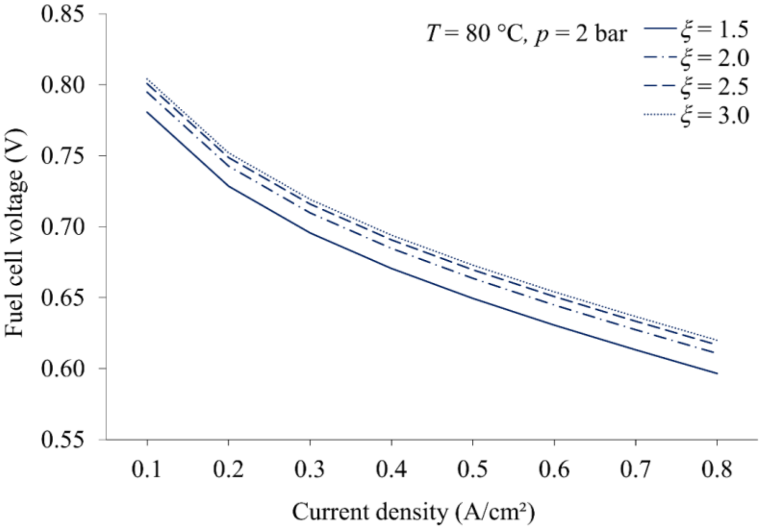
T = 80 °C, p = 2 bar
ξ = 1.5
ξ = 2.0
ξ = 2.5
ξ = 3.0
Fuel cell voltage (V)
0.85
0.80
0.75
0.70
0.65
0.60
0.55
0.1
0.2
0.3
0.4
0.5
0.6
0.7
0.8
Current density (A/cm²)

(a)

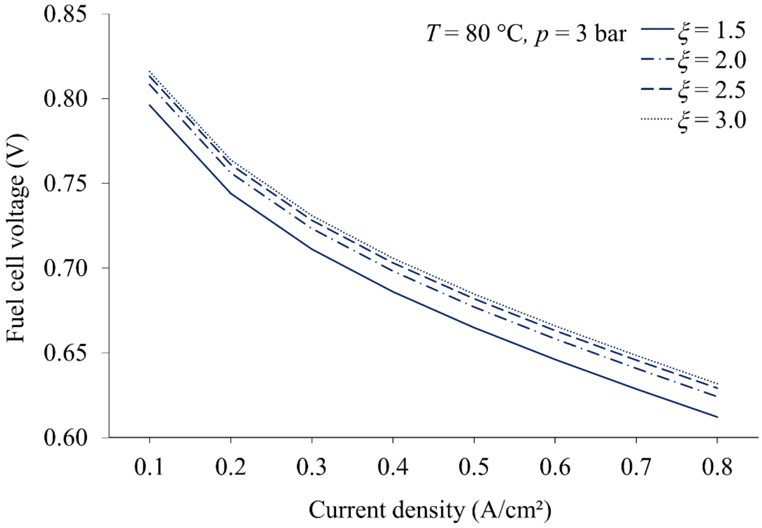
T = 80 °C, p = 3 bar
ξ = 1.5
ξ = 2.0
ξ = 2.5
ξ = 3.0
Fuel cell voltage (V)
0.85
0.80
0.75
0.70
0.65
0.60
0.1
0.2
0.3
0.4
0.5
0.6
0.7
0.8
Current density (A/cm²)

(b)

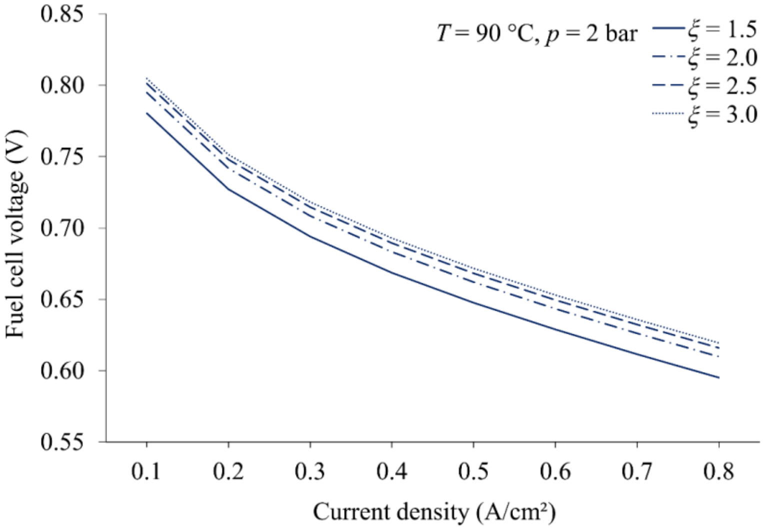
T = 90 °C, p = 2 bar
ξ = 1.5
ξ = 2.0
ξ = 2.5
ξ = 3.0
Fuel cell voltage (V)
0.85
0.80
0.75
0.70
0.65
0.60
0.55
0.1
0.2
0.3
0.4
0.5
0.6
0.7
0.8
Current density (A/cm²)

(c)

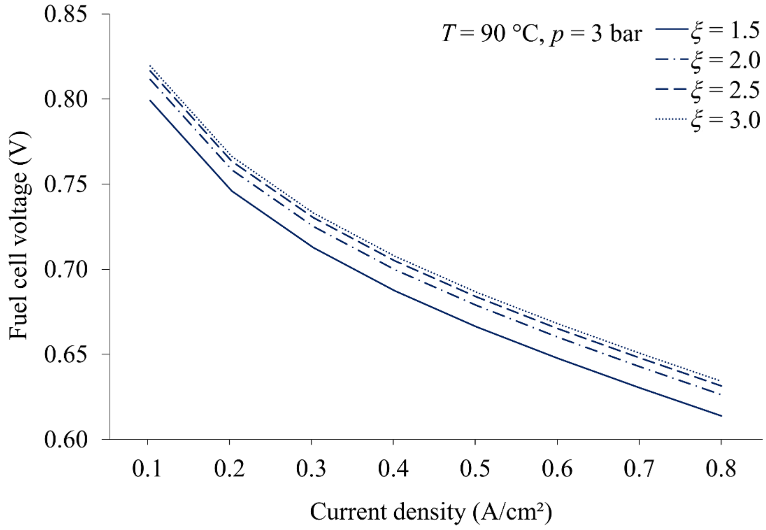

(d)

Figure 6. Polarization curves at different air stoichiometric rates: **a)** 80°C, 2 bar **b)** 80°C, 3 bar **c)** 90°C, 2 bar **d)** 90°C, 3 bar.

As can be seen from the polarization curves in Figure 6, fuel cell performance increases as the stoichiometric rate increases. Accordingly, in this study, it is seen that the best fuel cell performance will be achieved in case of the stoichiometric rate is 3. However, for a better fuel cell performance, optimum value of the air stoichiometric rate should be determined in order to provide required membrane humidity. Optimum value of the stoichiometric rate positively affects the fuel cell performance.

Air stoichiometric flow rate affects the amount of oxygen in the cell and humidity in the membrane. If this value is low, the amount of oxygen reaching the membrane decreases, which reduces the fuel cell’s performance. At the same time, the low value of this value increases the conductivity by increasing the moisture of the membrane. For this reason, it is essential to find the optimum value.

4. CONCLUSION

In this study, the performance changes of the PEM fuel cell were analyzed numerically using the MATLAB® program. In this model, the effects of fuel cell operating temperature, operating pressure, cathode pressure, and air stoichiometric rate on fuel cell performance were investigated. Analyses were made based on empirical equations and various physical facts and concluded that the parametric model is an excellent way to predict fuel cells’ performance.

- Working pressure increases the performance up to a certain value.
- Although the working pressure generally increases the performance, reaching high-pressure values is unnecessary. After 3 bar pressure, the increase in performance decreases and the possibility of leakage and membrane rupture due to high pressure increases. For this reason, 3 bar pressure was determined as the pressure limit.
- Although air stoichiometric rate makes a significant contribution to performance, higher values have a negative effect.

Fuel cell power output variation was determined using optimum values that are found in this study. Values to be used to maximize fuel cell efficiency have been found as a result of electrochemical modeling and power output values are shown in Fig. 7.

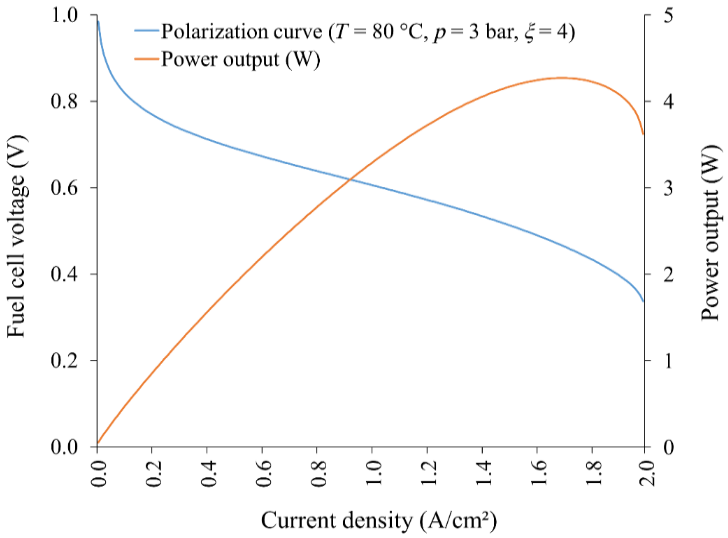

Figure 7. Variation of fuel cell voltage and fuel cell power output with the current density at the optimum operating conditions.

As can be seen from Fig. 7, the fuel cell power output, obtained for the optimum values of the operating parameters, reaches its maximum level at a certain value of the voltage. In this study, maximum value of power output was obtained approximately 4.27 W at a value of about 0.47 V.

Analyses can improve the design by obtaining the necessary preliminary information for the fuel cell and cooling system design. A good cooling system design will have an enormous impact on FC performance. The practical system could be improved with the information that is given by the study. It was emphasized that temperature might be an essential change in future studies. Besides, the controlled changing of the parameters in the study can be analyzed from different variables.

NOMENCLATURE

A	Ampere meter, or area (cm²)
c'	Concentration of gas (mol/cm^3)
ΔG°	Gibbs free energy change (J)
F	Faraday's constant (C/mol)
i	Current (A)
j	Current density (A/cm²)
l	Thickness (cm)
ne	Number of electrons
p	Pressure (bar)
PEM	Proton Exchange Membrane
PEMFC	Proton Exchange Membrane Fuel Cell
R	Universal gas constant J/(mol·K), or resistivity (Ω)
T	Temperature (K)
V	Voltage (V)
x	Dry gas ratio
χ	Molar ratio
ξ	Stoichiometric rate

Subscript

A	Anode
act	Activation
conc	Concentration
C	Cathode
FC	Fuel Cell
gen	Generation
HHV	High Heating Value
int	Internal
irrev	Irreversible
L	Limited
mem	Membrane
rev	Reversible
sat	Saturation

DECLARATION OF ETHICAL STANDARDS

The authors of the paper submitted declare that nothing which is necessary for achieving the paper requires ethical committee and/or legal-special permissions.

CONTRIBUTION OF THE AUTHORS

Kemal Bilen: Supervised the related master's thesis and wrote the manuscript.

Batukan Cem Tarhan: Performed the numerical analysis and formed the graphs.

Selahattin Çelik: Interpreted the obtained graphics and results.

CONFLICT OF INTEREST

The authors acknowledge that there is no known conflict of interest or common interest with any institution/organization or person.

REFERENCES

[1] Stolten D, Emonts B. Hydrogen Science and Engineering: Materials, Processes, Systems and Technology. Wiley-VCH, 2016.

[2] Colpan CO, Nalbant Y, Ercelik M. Fundamentals of fuel cell technologies, in: Comprehensive Energy Systems, Elsevier Incorporation, 2018: 1107-1130.

[3] Srinivasan S. Fuel cells: From fundamentals to applications. 2006.

[4] Thomas JM, Edwards PP, Dobson PJ, Owen G. Decarbonising energy: The developing international activity in hydrogen technologies and fuel cells. Journal of Energy Chemistry 2020; 51: 405-415.

[5] Sundén B. Chapter 11 - Fuel cell systems and applications, in: B.B.T.-H. Sundén Batteries and Fuel Cells (Ed.), Academic Press 2019: 203-216.

[6] Li X, Sabır I, Review of bipolar plates in PEM fuel cells: Flow-field designs. International Journal of Hydrogen Energy 2005; 30(4): 359-371.

[7] Ültanır MÖ. 21. yüzyıla girerken Türkiye'nin enerji stratejisinin değerlendirilmesi, TÜSİAD, 1998.

[8] Yilmaz AE, Ispirli MM. An investigation on the parameters that affect the performance of hydrogen fuel cell. Procedia-Social and Behavioral Sciences 2015; 195: 2363-2369.

[9] Ye YS, Rick J, Hwang BJ. Water soluble polymers as proton exchange membranes for fuel cells. Polymers 2012; 4(2): 913-963.

[10] Sankar K, Aguan K, Jana AK. A proton exchange membrane fuel cell with an airflow cooling system: Dynamics, validation and nonlinear control. Energy Conversion and Management 2019; 183: 230-240.

[11] Faghri A, Guo Z. Integration of heat pipe into fuel cell technology. Heat Transfer Engineering 2008; 29: 232-238.

[12] Choi EJ, Park JY, Kim MS. Two-phase cooling using HFE-7100 for polymer electrolyte membrane fuel cell application. Applied Thermal Engineering 2019; 148: 868-877.

[13] Afshari E, Ziaei-Rad M, Dehkordi MM. Numerical investigation on a novel zigzag-shaped flow channel design for cooling plates of PEM fuel cells. Journal of the Energy Institute 2017; 90: 752-763.

[14] Han J, Park J, Yu S. Control strategy of cooling system for the optimization of parasitic power of automotive fuel cell system. International Journal of Hydrogen Energy 2015; 40: 13549-13557.

[15] Hajmohammadi MR, Toghraei I. Optimal design and thermal performance improvement of a double-layered microchannel heat sink by introducing Al_2O_3 nano-particles into the water. Physica A: Statistical Mechanics and its Applications 2018; 505: 328-344.

[16] Yu S, Jung D. A study of operation strategy of cooling module with dynamic fuel cell system model for transportation application. Renewable Energy 2010; 35: 2525-2532.

[17] Saygili Y, Eroglu I, Kincal S. Model based temperature controller development for water cooled PEM fuel cell systems. International Journal of Hydrogen Energy 2015; 40: 615-622.

[18] Fronk MH, Wetter DL, Masten DA, Bosco A. PEM fuel cell system solutions for transportation. SAE Transaction 2000; 109: 212-219.

[19] Nguyen C, Roy G, Galanis N, Suiro S. Heat transfer enhancement by using Al_2O_3-water nanofluid in a liquid cooling system for microprocessors. Proceeding 4th WSEAS International Conference of Heat Transfer Thermal Engineering Environment Elounda, Greece 2006: 103-108.

[20] Rahimi S, Meratizaman M, Monadizadeh S, Amidpour M. Techno-economic analysis of wind turbine-PEM (polymer electrolyte membrane) fuel cell hybrid system in standalone area. Energy 2014; 67: 381-396.

[21] Mert SO, Dincer I, Ozcelik Z. Performance investigation of a transportation PEM fuel cell system. International Journal of Hydrogen Energy 2012; 37: 623-633.

[22] Zafar S, Dincer I. Energy, exergy and exergoeconomic analyses of a combined renewable energy system for residential applications. Energy Buildings 2014; 71: 68-79.

[23] Mann RF, Amphlett JC, Hooper MAI, Jensen HM, Peppley B., Roberge PR. Development and application of a generalized steady-state electrochemical model for a PEM fuel cell. Journal of Power Sources 2000; 86: 173-180.

[24] Musio F, Tacchi F, Omati L, Stampino PG, Dotelli G, Limonta S, Brivio D, Grassini P. PEMFC system simulation in MATLAB-Simulink® environment. International Journal of

Hydrogen Energy 2011; 36: 8045-8052.

[25] Miansari M, Sedighi K, Amidpour M, Alizadeh E, Miansari M. Experimental and thermodynamic approach on proton exchange membrane fuel cell performance. Journal of Power Sources 2009; 190: 356-361.

[26] Rowe A, Li X. Mathematical modeling of proton exchange membrane fuel cells. Journal of Power Sources 2001; 102: 82-96.

[27] Amphlett JC, Baumert RM, Mann RF, Peppley BA, Roberge PR, Harris TJ. Performance Modeling of the Ballard Mark IV Solid Polymer Electrolyte Fuel Cell I. Mechanistic Model Development Physical Properties, Assumptions, and Approximations, 1995.

[28] Spiegel C. Chapter 5 - Fuel Cell Mass Transport, in: C. Spiegel (Ed.), PEM Fuel Cell Model. Simulation Using MATLAB®. Academic Press, Burlington 2008; 97-125.

[29] Barbir F. 3. Fuel Cell Electrochemistry. PEM Fuel Cells 2005; 33-72.

[30] Laurencelle F, Chahine R, Hamelin J, Agbossou K, Fournier M, Bose TK, Laperrière A. Characterization of a Ballard MK5-E proton exchange membrane fuel cell stack. Fuel Cells 2001; 1: 66-71.

[31] Tohidi M, Mansouri SH, Amiri H. Effect of primary parameters on the performance of PEM fuel cell. International Journal of Hydrogen Energy, Pergamon 2010: 9338-9348.

[32] Yan Q, Toghiani H, Causey H. Steady state and dynamic performance of proton exchange membrane fuel cells (PEMFCs) under various operating conditions and load changes. Journal of Power Sources 2006; 161: 492-502.

[33] Cellek M, Bilgili M. Stokiyometri oranının iki hücreli PEM yakıt hücresi yığını performansına etkisinin incelenmesi. Gazi University Journal of Science Part C: Design and Technology 2021; 9(1): 134-147.